

# Insights into mobile genetic elements and the role of conjugative plasmid in transferring aminoglycoside resistance in extensively drug-resistant *Acinetobacter baumannii* AB329 (#73306)

1

First submission

## Guidance from your Editor

Please submit by **24 May 2022** for the benefit of the authors (and your \$200 publishing discount) .



### Structure and Criteria

Please read the 'Structure and Criteria' page for general guidance.



### Custom checks

Make sure you include the custom checks shown below, in your review.



### Raw data check

Review the raw data.



### Image check

Check that figures and images have not been inappropriately manipulated.

Privacy reminder: If uploading an annotated PDF, remove identifiable information to remain anonymous.

## Files

Download and review all files from the [materials page](#).

4 Figure file(s)

1 Raw data file(s)

## ! Custom checks

### DNA data checks

- ! Have you checked the authors [data deposition statement](#)?
- ! Can you access the deposited data?
- ! Has the data been deposited correctly?
- ! Is the deposition information noted in the manuscript?




# Structure and Criteria

## Structure your review

The review form is divided into 5 sections. Please consider these when composing your review:

1. BASIC REPORTING
2. EXPERIMENTAL DESIGN
3. VALIDITY OF THE FINDINGS
4. General comments
5. Confidential notes to the editor






 You can also annotate this PDF and upload it as part of your review

When ready [submit online](#).





## Editorial Criteria

Use these criteria points to structure your review. The full detailed editorial criteria is on your [guidance page](#).

### BASIC REPORTING

-  Clear, unambiguous, professional English language used throughout.
-  Intro & background to show context. Literature well referenced & relevant.
-  Structure conforms to [Peerj standards](#), discipline norm, or improved for clarity.
-  Figures are relevant, high quality, well labelled & described.
-  Raw data supplied (see [Peerj policy](#)).

### EXPERIMENTAL DESIGN

-  Original primary research within [Scope of the journal](#).
-  Research question well defined, relevant & meaningful. It is stated how the research fills an identified knowledge gap.
-  Rigorous investigation performed to a high technical & ethical standard.
-  Methods described with sufficient detail & information to replicate.

### VALIDITY OF THE FINDINGS

-  Impact and novelty not assessed. *Meaningful* replication encouraged where rationale & benefit to literature is clearly stated.
-  All underlying data have been provided; they are robust, statistically sound, & controlled.
-  Conclusions are well stated, linked to original research question & limited to supporting results.



The best reviewers use these techniques

## Tip

## Example

**Support criticisms with evidence from the text or from other sources**

*Smith et al (J of Methodology, 2005, V3, pp 123) have shown that the analysis you use in Lines 241-250 is not the most appropriate for this situation. Please explain why you used this method.*

**Give specific suggestions on how to improve the manuscript**

*Your introduction needs more detail. I suggest that you improve the description at lines 57- 86 to provide more justification for your study (specifically, you should expand upon the knowledge gap being filled).*

**Comment on language and grammar issues**

*The English language should be improved to ensure that an international audience can clearly understand your text. Some examples where the language could be improved include lines 23, 77, 121, 128 – the current phrasing makes comprehension difficult. I suggest you have a colleague who is proficient in English and familiar with the subject matter review your manuscript, or contact a professional editing service.*

**Organize by importance of the issues, and number your points**

1. Your most important issue
2. The next most important item
3. ...
4. The least important points

**Please provide constructive criticism, and avoid personal opinions**

*I thank you for providing the raw data, however your supplemental files need more descriptive metadata identifiers to be useful to future readers. Although your results are compelling, the data analysis should be improved in the following ways: AA, BB, CC*

**Comment on strengths (as well as weaknesses) of the manuscript**

*I commend the authors for their extensive data set, compiled over many years of detailed fieldwork. In addition, the manuscript is clearly written in professional, unambiguous language. If there is a weakness, it is in the statistical analysis (as I have noted above) which should be improved upon before Acceptance.*

# Insights into mobile genetic elements and the role of conjugative plasmid in transferring aminoglycoside resistance in extensively drug-resistant *Acinetobacter baumannii* AB329

Supat Kongfak<sup>1</sup>, Rapee Thummeepak<sup>1</sup>, Udomluk Leungtongkam<sup>1</sup>, Kannipa Tasanapak<sup>1</sup>, Aunchalee Thanwisai<sup>1</sup>, Sutthirat Sitthisak<sup>Corresp. 1, 2</sup>

<sup>1</sup> Department of Microbiology and Parasitology, Faculty of Medical Science, Naresuan University, Muang, Phitsanulok, Thailand

<sup>2</sup> Centre of Excellence in Medical Biotechnology, Faculty of Medical Science, Naresuan University, Muang, Phitsanulok, Thailand

Corresponding Author: Sutthirat Sitthisak  
Email address: Sutthirats@nu.ac.th

*Acinetobacter baumannii* is a major cause of nosocomial infection and incidence of extensively drug-resistant *A. baumannii* (XDRAB) infections has dramatically increased worldwide. In this study, we aimed to explore the complete genome sequence of XDRAB 329, ST1166/98 (Oxford/Pasteur), which is an outbreak clone from a hospital in Thailand. Whole-genome sequencing (WGS) was performed on short-read Illumina and long-read PacBio sequencing, and a conjugation assay of its plasmid was performed. The complete genome sequence of AB329 revealed a circular chromosome of 3,948,038 bp in length with 39% GC content. Antibiotic resistance genes (ARGs) including beta-lactam resistance (*bla*OXA-51, *bla*ADC-25, *bla*OXA-23, *bla*TEM-1D), aminoglycoside resistance (*aph*(3')-Ia, *aph*(3')-Ib, *aph*(6)-Id, *armA*), tetracycline resistance (*tet*(B), *tet*(R)), macrolide resistance (*mph*(E), *msr*(E)), and efflux pumps were found. Mobile genetic elements (MGEs) of AB329 revealed two plasmids (pAB329a and pAB329b), three prophages, 19 genomic islands (GIs), and 33 insertion sequences (ISs). pAB329a is a small circular plasmid with 8,731 bp, and pAB329b is a megaplasmid with 82,120 bp. *aph*(3')-Ia were detected in pAB329b, and major facilitator superfamily (MFS) transporter was detected in the prophage. *Acinetobacter baumannii* resistance island 4 (AbaR4) harboring tetracycline and aminoglycoside resistance was detected in the genome of AB329. pAB329b, which belonged to Rep type GR6 (plasmid lineage LN\_1), was a conjugative plasmid with the ability to transfer aminoglycoside resistance gene to sodium azide-resistant *A. baumannii*. This study provides insights into the feature of the MGEs of XDRAB, which are the main reservoir and source of dissemination of ARGs.

# Abstract

*Acinetobacter baumannii* is a major cause of nosocomial infection and incidence of extensively drug-resistant *A. baumannii* (XDRAB) infections has dramatically increased worldwide. In this study, we aimed to explore the complete genome sequence of XDRAB 329, ST1166/98 (Oxford/Pasteur), which is an outbreak clone from a hospital in Thailand. Whole-genome sequencing (WGS) was performed on short-read Illumina and long-read PacBio sequencing, and a conjugation assay of its plasmid was performed. The complete genome sequence of *A. baumannii* AB329 revealed a circular chromosome of 3,948,038 bp in length with 39% GC content. Antibiotic resistance genes (ARGs) including beta-lactam resistance (*bla*<sub>OXA-51</sub>, *bla*<sub>ADC-25</sub>, *bla*<sub>OXA-23</sub>, *bla*<sub>TEM-1D</sub>), aminoglycoside resistance (*aph*(3')-Ia, *aph*(3'')-Ib, *aph*(6)-Id, *armA*), tetracycline resistance (*tet*(B), *tet*(R)), macrolide resistance (*mph*(E), *msr*(E)), and efflux pumps were found. Mobile genetic elements (MGEs) of *A. baumannii* AB329 revealed two plasmids (pAB329a and pAB329b), three prophages, 19 genomic islands (GIs), and 33 insertion sequences (ISs). pAB329a is a small circular plasmid with 8,731 bp, and pAB329b is a megaplasmid with 82,120 bp. *aph*(3')-VIa were detected in pAB329b, and major facilitator superfamily (MFS) transporter was detected in the prophage. *Acinetobacter baumannii* resistance island 4 (AbaR4) harboring tetracycline and aminoglycoside resistance was detected in the genome of *A. baumannii* AB329. pAB329b, which belonged to Rep type GR6 (plasmid lineage LN\_1), was a conjugative plasmid with the ability to transfer aminoglycoside resistance gene to sodium azide-resistant *A. baumannii*. This study provides insights into the feature of the MGEs of XDRAB, which are the main reservoir and source of dissemination of ARGs.

24

## 25 Introduction

26 *Acinetobacter baumannii* is a bacterium that is a major cause of nosocomial infection,  
 27 especially in intensive care units (ICUs). In the past decades, the prevalence of  
 28 extensively drug-resistant *A. baumannii* (XDRAB) has been rapidly increasing  
 29 worldwide. Numerous antibiotic resistance genes (ARGs) were detected in the genomes  
 30 and mobile genetic elements (MGEs) of XDRAB, and they were found to be responsible  
 31 for the spread of antibiotic resistance. A variety of MGEs has been described in *A.*  
 32 *baumanni*. **In silico** analysis detected various ARGs located in *A. baumannii* conjugative  
 33 plasmids (*Makke et al., 2020; Martins-Sorenson et al., 2020*). To date, plasmid  
 34 classification for *A. baumannii* is done based on the homology of Rep proteins, which  
 35 are divided into 23 different groups (GR1-23) (*Salgado-Camargo et al., 2020*). In  
 36 addition, a conjugative plasmid in *A. baumannii* was classified into 21 lineages based on  
 37 their backbone homology (*Salgado-Camargo et al., 2020*). The conjugative plasmid  
 38 requires the origin of transfer and the *tra* operon, which is important for generating the  
 39 F-pilus that is needed for transferring genetic materials. The *tra* genes are detected and  
 40 associated with plasmid GR6, which is classified using the replicon typing (AB-PBRT)  
 41 method (*Kongthai et al., 2021*). These plasmid groups are responsible for the  
 42 dissemination of drug resistance genes such as *bla*<sub>OXA-23</sub> and *aphA6* (*Saranathan et al.,*  
 43 *2014; Leungtonkam et al., 2018a*). Prophages are MGEs that constitute 10–20% of a  
 44 bacterium's genome and provide new genetic information such as virulence factors and  
 45 drug resistance mechanisms (*Casjens, 2003*). The number of prophages identified in  
 46 the 177 *A. baumannii* genomes range from 1 to 15, and less than 5% of the deposited

sequence contains the prophage-encoded ARGs (Loh et al., 2020). AbaR-type genomic islands (AbaRs) are important elements responsible for antimicrobial resistance in *A. baumannii*. Several AbaRs were characterized, and the majority, such as AbaR1, AbaR3, AbaR5, AbaR6, AbaR7, AbaR8, AbaR9, and AbaR10, were identified in epidemic clones like international clone (IC) 1 (Pagano, Martins & Barth, 2016). Others were identified in IC II such as AbaR4 (Kim, Park & Ko, 2012). Other MGES such as integrons, transposons, and insertion sequences (ISs) were also found to be related to antibiotic resistance in *A. baumannii*. The main MGEs associated with resistance are ISAba1 (*bla*<sub>OXA-23</sub>, *bla*<sub>OXA-5</sub>, *bla*<sub>OXA-58</sub>, *bla*<sub>AmpC</sub>), ISAba2 (*bla*<sub>OXA-58</sub>, *bla*<sub>AmpC</sub>), ISAba3 (*bla*<sub>OXA-58</sub>), ISAba4 (*bla*<sub>OXA-23</sub>), ISAba10 (*bla*<sub>OXA-23</sub>), ISAba125 (*bla*<sub>NDM-1</sub>, *bla*<sub>NDM-2</sub>, *bla*<sub>AmpC</sub>, *aphA6*), IS18 (*bla*<sub>OXA-58</sub>), Tn2006 (*bla*<sub>OXA-23</sub>), Tn2007 (*bla*<sub>OXA-23</sub>), Tn2008 (*bla*<sub>OXA-23</sub>), Int1 (*bla*<sub>GES-11</sub>, *bla*<sub>GES-14</sub>, *dfrA1*, *sat2*, *aadA1*, *orfX*, *ybfA*, *ybfB*), and Int2 (*dfrA1*, *sat2*, *aadA1*, *orfX*, *ybfA*, *ybfB*, *ybgA*) (Pagano, Martins & Barth, 2016; Turton et al., 2006; Bahador et al., 2015; Joshi et al., 2017). In addition, different ISs located upstream and/or downstream of ARGs increase the transcription of the ARGs.

*A. baumannii* clonal outbreak belonged to three international groups, and IC 2 is the predominant clonal lineage in Asia, including in Thailand (Kim et al., 2013). Our previous study of 339 *A. baumannii* isolates collected from four hospitals in Thailand revealed 7.9% of XDRAB among the total isolates collected (Leungtonkam et al., 2018a). We found an outbreak clone of XDRAB in one hospital with the same ST type and plasmid group, and it belonged to IC 2 (Kongthai et al., 2021). All of them were ST1166/98 (Oxford/Pasteur) that contained plasmid groups 2 and 6. Little is known about the role of conjugative plasmid in the functioning of XDRAB. The use of whole-

genome sequencing (WGS) technology can assist in tackling antimicrobial resistance, virulence determinance, and MGEs in *A. baumannii* (Makke et al., 2020; Martins-Sorenson et al., 2020). Combined with short- and long-read sequencing, WGS will be able to resolve an accurate and complete genome and plasmid structure. Thus, this study aimed to obtain the complete genome sequence of one XDRAB and characterized the MGEs and the role of its plasmid in transferring the ARG.

## Materials and Methods

### Bacterial strains and antibiotic susceptibility testing

*A. baumannii* AB329, which is a phage-susceptible XDRAB strain, was isolated from patient sputum obtained from our previous study (Leungtongkam et al., 2018a). This is a representative of the outbreak clone obtained from a hospital in east Thailand, and it was collected from November 2013 to February 2015 (Leungtongkam et al., 2018a). Antimicrobial susceptibility testing was performed as previously described (Kongthai et al., 2021). The protocol was approved by Naresuan University Institutional Biosafety Committee, and the project number was NUIBC MI 63-07-21.

### Polymerase chain reaction (PCR)-based plasmid typing

The PCR-based method was used to detect plasmid groups (GRs) with primers specific to each GR from GR1 to GR19, which were described by a previous study (Bertini et al., 2010).

### DNA extraction, genome sequencing and assembly

Genomic DNA of *A. baumannii* AB329 was extracted using the Real Genomics DNA Extraction Kit (RBC Biosciences, Taiwan), and it was quantified using a Qubit® DNA Assay Kit in Qubit® 2.0 Fluorometer (Life Technologies, CA, USA) prior to sequencing

with both short-read (Illumina paired-end) and long-read (PacBio, Menlo Park, CA, USA) sequencing systems. For short-read sequencing, paired-end sequencing libraries (2 × 250 bp) were constructed using the Nextera XT sample preparation kit following the manufacturer's suggestions, and they were sequenced using the Illumina MiSeq platform. The Illumina reads were trimmed with Sickle v1.33 using the default parameters (Joshi & Fas, 2011). For long-read sequencing, a large insert library (10 kb) was constructed and sequenced on the PacBio RS platform (Pacific Biosciences, Menlo Park, CA, USA). A hybrid assembly was conducted with the Illumina trimmed reads and PacBio reads using Unicycler v0.4.8.0 with the default settings (Wick et al., 2017). Unicycler automatically identified and trimmed the overlapping ends, and circular sequences were rotated to *dnaA*.

# Genome annotation and bioinformatic analysis

The assembled circular chromosome and plasmids were functionally annotated using Prokka v1.12 with the default options (Seemann, 2014). The complete genomes of 292 *A. baumannii* strains retrieved from the NCBI database in December 2021 were used to identify the core genome (Table S1). A single-nucleotide polymorphisms (SNPs) phylogenetic tree of core genome was reconstructed using CSI Phylogeny with the default settings (Kaas et al., 2014). This tree was visualized and edited using Interactive Tree of Life (iTOL) (<https://itol.embl.de/>). A pan-genomic analysis was executed using Roary v.3.13.0, which compared with five closest relative genomes including *A. baumannii* NIPH17\_00019 (AP024415.1), *A. baumannii* XH856 (CP014541.1), *A. baumannii* KAB02 (CP017644.1), *A. baumannii* KAB06 (CP017652.1) and *A. baumannii* KAB05 (CP017650.1). Then, the output was illustrated using R studio as described in

[https://github.com/lamlaml/pADAP\\_project/tree/master/Roary\\_stats](https://github.com/lamlaml/pADAP_project/tree/master/Roary_stats). The average nucleotide identity (ANI) was calculated using FastANI v.1.3 to estimate whole genome similarity among the two XDRAB strains, which were obtained from hospitalized patients in Thailand (*Kongthai et al., 2021*), and the five closest relative genomes identified from the pan-genomic analysis. Antimicrobial resistance and virulence genes were retrieved using the Comprehensive Antibiotic Resistance Database (CARD) (<https://card.mcmaster.ca/>) and VFAnalyzer (*Liu et al., 2019*), respectively. The large-scale BLAST score ratio (LS-BSR) pipeline was utilized to compare the virulence and drug resistance genes with 292 *A. baumannii* genomes (*TableS1*). A BSR value of 0.4 and above was interpreted as the presence of genes, and a BSR value below 0.4 was inferred as gene absence (*Sahl et al., 2014; Yakkala et al., 2019*). Then, these BSR values were used to build a hierarchical clustering heat map using the R packages; pheatmap and tidyverse. MGEs were detected using MobileElementFinder (*Johansson et al., 2021*). The presence of prophage sequences in the genome of the *A. baumannii* AB329 was analyzed using the PHAge Search Tool Enhanced Release (PHASTER) online server (*Arndt et al., 2016*). Prophage open reading frames (ORFs) were examined as described in a previous study (*Fu et al., 2017*). The presence of genomic islands (GIs) was performed as described previously (*Thummeepak et al., 2020*), and the GIs identified in *A. baumannii* ACICU used nucleotide queries (*Di Nocera et al., 2011*). Plasmid comparison and the identification of the AbaR structure were accomplished using Easyfig version 2.1 (*Sullivan, Petty & Beatson, 2011*). The complete genome was deposited in the NCBI GenBank database under accession numbers CP091452 (chromosome), CP091453 (pAB329a), and CP091454 (pAB329b).

# Conjugation experiment

Broth-mating conjugation assay was performed according to previously published protocol with minor modifications (Leungtongkam et al., 2018b). Overnight cultures of the donor (*A. baumannii* AB329) and the recipient *A. baumannii* NU13R) were adjusted in 0.85% NaCl until the cell suspensions reached the turbidity equal to a McFarland value of 0.5, which was measured using a densitometer (SiaBiosan, Riga, Latvia). Equal volumes (250 µl) of adjusted cell suspensions of the donor and the recipient were mixed in 500 µl of 2× Luria-Bertini (LB) broth and incubated for 4 h at 37°C. Transconjugants were selected on LB plates containing the following components: 250 µg/ml sodium azide; 50 µg/ml ticarcillin or 250 µg/ml sodium azide; 20 µg/ml kanamycin. The conjugation frequency (CF) was calculated as previously described (Leungtongkam et al., 2018b).

# Results

## Antibiotic susceptibility and complete genome sequence of *A. baumannii* AB329

The study of the antibiotic susceptibility of *A. baumannii* AB329 showed that it is resistant to amikacin (AK), cefotaxime, ceftazidime, ceftriaxone, cefepime, ciprofloxacin, gentamicin, imipenem, meropenem, trimethoprim/sulfamethoxazole, tetracycline, and piperacillin/tazobactam (TableS2) but is still susceptible to colistin (Minimum inhibitory concentrations (MIC) 1 ug/mL) and tigecycline (MIC 0.25 ug/mL). The complete genome sequence of *A. baumannii* AB329 generated by short- and long-read sequencing revealed a circular chromosome of 3,948,038 bp in length with 39% GC content, and it contained two plasmids (pAB329a and pAB329b) (Table 1). The Prokka prokaryotic genome annotation system identified 18 rRNAs, 72 tRNAs, 3,837 ORFs, and a total of

3,569 protein-coding genes on the main chromosome of AB329 (Table S3). AB329 was assigned to MLST type 1166/98 (Oxford/ Pasteur) and was found to belong to a lineage of IC 2.

### Phylogenomic and comparative genomic analysis of *A. baumannii* AB329

Phylogenomic analysis was performed using the core genome of *A. baumannii* AB329 and the additional 292 *A. baumannii* strains deposited in the NCBI database. As shown in Figure 1A, phylogenetic analysis of *A. baumannii* AB329 presented in the same cluster with the *A. baumannii* strains NIPH17\_00019 (AP024415.1), XH856 (CP014541.1), KAB02 (CP017644.1), KAB06 (CP017652.1), and KAB05 (CP017650.1), respectively (Figure 1B and Table S4). We also compared the genome of *A. baumannii* AB329 with two XDRAB isolated from two different hospitals in Thailand as previously described (Kongthai et al., 2021). The ANI (%) of *A. baumannii* AB329 with *A. baumannii* AB140 and *A. baumannii* AB053 was 99.72 % and 99.27 %, respectively. A pan-genome of *A. baumannii* AB329 consisting of 4,628 genes represented the core, shell, and cloud genomes, respectively (Figure 2B). The core genome represents a pool of conserved genes, which are present in all genomes including 3,238 genes. The accessory genes, which were shell genes and cloud genes, constituted a total of 1,390 genes.

### Virulence genes, antibiotic resistance genes, and mobile genetic elements of *A. baumannii* AB329

Analysis of the virulence genes of *A. baumannii* AB329 revealed that genes were involved in iron uptake (*hemO*, *barA*, *barB*, *basA*, *basB*, *basC*, *basD*, *basF*, *basG*, *bash*, *basI*, *basJ*, *bauA*, *bauB*, *bauC*, *bauD*, *bauE*, *bauF*, *entE*), serum resistance (*pbpG*),

185 stress adaptation (*katG*, *katE*), gene regulation (*bfmR*, *bfmS*), immune evasion (*lpsB*,  
186 *lpxA*, *lpxB*, *lpxC*, *lpxD*, *lpxL*, *lpxM*), enzyme phospholipase (*plcC*, *plcD*), biofilm  
187 formation (*adeF*, *adeG*, *adeH*, *csuA*, *csuB*, *csuC*, *csuD*, *csuE*, *pgaA*, *pgaB*, *pgaC*,  
188 *pgaD*), and host cell adherence (*ompA*) (Figure 2A). Resistome analysis detected a  
189 number of resistance mechanisms in the chromosome, including beta-lactam-  
190 inactivating enzymes, aminoglycoside-modifying enzymes, efflux pumps, permeability  
191 defects, and target site modifications. As shown in Figure 2B, the genes conferring drug  
192 resistance, including beta-lactam resistance (*bla*<sub>OXA-51</sub>, *bla*<sub>ADC-25</sub>, *bla*<sub>OXA-23</sub>, *bla*<sub>TEM-1D</sub>),  
193 aminoglycoside resistance (*aph*(3')-Ia, *aph*(3'')-Ib, *aph*(6)-Id, *armA*), tetracycline  
194 resistance (*tet*(B), *tet*(R)), and macrolide resistance (*mph*(E), *msr*(E)) were detected in  
195 the chromosome. Genes encoding resistance-nodulation-cell division (RND) (*AdeABC*,  
196 *AdeIJK*, and *AdeFGH*), multidrug and toxic efflux (MATE) (*AbeM*), major facilitator  
197 superfamily (MFS) (*tet*(A) and *tet*(B)), and small multidrug resistance (SMR) efflux  
198 systems (*AbeS*) were found. In silico analysis of the pattern of ARGs was conducted,  
199 and the 292 selected *A. baumannii* genomes worldwide were grouped into three  
200 clusters (A, B, and C) (Figure 2B). We found that *A. baumannii* AB329 were grouped  
201 into cluster C and closely related to *A. baumannii* VB2181(CP050401.1) and AC29  
202 (CP007535.2), which were isolated from India and Malaysia, respectively. The MGEs of  
203 *A. baumannii* AB329 revealed two plasmids, three prophages, 19 GIs, and 33 ISs. The  
204 two plasmids were pAB329a and pAB329b. pAB329a is a small circular plasmid with  
205 8,731 bp, and pAB329b is a mega plasmid with 82,120 bp. pAB329b carries  
206 conjugation-gene clusters required for autonomous conjugative transfer, which involves  
207 F pilus (*traD*, *traE*, *traK*, *traB*, *traV*, *traC*, *traW*, *traN*, *traF*, *traH*, *traG*, *traW*), plasmid

208 replication (*repA*), and a recombinase (*recD2*). A few hypothetical proteins and one  
 209 copy of the aminoglycoside resistance gene *aph(3')*-Vla were detected in pAB329b  
 210 (Figure 3A). The genomic features of plasmid pAB329b aligned with 11 closely relative  
 211 plasmids deposited in the GenBank database as represented in Figure 3A. pAB329a  
 212 was closely related to plasmid p2AB5075 (CP008708.1) in lineage\_2(LN\_2), and  
 213 pAB329b was similar to pACICU2(NC\_010606) in LN-1 (Table S5). Compared to  
 214 pACICU2, we found that both plasmids have the same backbone regions; however,  
 215 pAB329b harbored the *aph(3')*-Vla gene, while in pACICU2, the ARG was absent  
 216 (Figure 3B). We found three prophages in the genome of *A. baumannii* AB329: one  
 217 intact and two incomplete prophages. Our bioinformatic analysis revealed that the intact  
 218 prophage sequence contained 69 ORFs involved in the DNA process, drug resistance,  
 219 host lysis, integrase, metabolism process, and phage proteins (Figure 4A). Interestingly,  
 220 the MFS transporter was detected in the genome of this prophage. The genome of this  
 221 prophage homology to *Acinetobacter* phage YMC11/11/R3177 (KP861230.1) with 57.98  
 222 % ANI. The genome of *A. baumannii* AB329 was examined for GIs, and 19 GIs were  
 223 identified (Table S6). In addition, one resistance island, AbaR4, which harbored  
 224 tetracycline and aminoglycoside resistance genes was detected in the genome of *A.*  
 225 *baumannii* AB329 (Figure 4B). Transposable elements such as transposons and ISs  
 226 were investigated, and 34 ISs were detected in the chromosome except for *ISAb*1,  
 227 which was detected in the chromosome and the plasmid (Table 1). *ISAb*125 was  
 228 detected only in the plasmid, and it bracketed the ARG *aph(3')*-Vla (Figure 3A). ARGs in  
 229 the chromosome located near the ISs are *bla*<sub>OXA-23</sub> (*ISAb*1), *bla*<sub>TEM</sub> (*ISAb*33), and  
 230 *aph(3')*-Vla ((*IS*6).

## Conjugative transfer of aminoglycoside resistance gene of plasmid pAB329b

To investigate the role of pAB329b in the transfer of the ABO resistance gene, we performed a conjugation assay to study the plasmid ability to transfer the aminoglycoside resistance gene to sodium azide-resistant *A. baumannii*, NU13R (recipient). As shown in Table 2, aminoglycoside resistance could be transferred from the donors (*A. baumannii* AB329) to the recipient (*A. baumannii* NU13R). The conjugation frequency was approximately  $1.2 \times 10^{-7}$ . The resistance genes, plasmid typing, and antibiotic susceptibility of the donors, the recipient, and the transconjugants are shown in Table 2.

## Discussion

The incidence of XDRAB infection has increased, resulting in hospital outbreaks worldwide, including in Thailand. In this study, we investigated the genome feature and MGEs of the XDRAB strain AB329. The complete genome sequence of *A. baumannii* AB329 was 3.9 Mb compared to that of previously reported XDRAB isolates, which ranged from 3.8 to 4.0 Mb (*Chopjitt et al., 2020; Si-Tuan et al, 2020; Makke et al., 2020*). The most dominant sequence type of Multidrug-resistance *A. baumannii* (MDRAB) in Thailand was found to be ST2 (Pasteur) belonging to IC2 (*Khuntayaporn et al., 2021; Chukamnerd et al., 2022*), and the XDRAB ST types reported in Thailand were ST2, 16, and 1479 (*Chopjitt et al., 2020; Kongthai et al., 2021*). We found that the ST type of the *A. baumannii* AB329 strain was ST98 (Pasteur). To date, the ST98 clone has been detected in the Carbapenem-resistant *A. baumannii* (CRAB) CRAB strain isolated from Portugal (*Silva et al., 2021*). An analysis of the clonal relationship of *A. baumannii* AB329 among 292 *A. baumannii* isolated worldwide (TableS2) revealed the

highest genome similarity with the *A. baumannii* strains KAB02 (CP017644.1), KAB05 (CP017650.1), and (CP017652.1) isolated from South Korea. These bacterial strains might share a common ancestor, and we speculated that *A. baumannii* KAB02, *A. baumannii* KAB05, and *A. baumannii* KAB06 might have been originated from *A. baumannii* AB329 since the genome size of *A. baumannii* AB329 was smaller than those of *A. baumannii* KAB02, *A. baumannii* KAB05, and *A. baumannii* KAB06 and *A. baumannii* AB329 was isolated before those strains. All ARGs were detected in the chromosome except the *aph(3')-VIa* gene found in the pAB329b. These results implied that the ARGs can be rapidly transferred or passed from parent to offspring and cause the outbreak clone in the hospital. The antibiotic susceptibility pattern of *A. baumannii* AB329 revealed high resistance to many beta-lactam antibiotics (Table S2). We detected only *bla*<sub>OXA-51</sub>, *bla*<sub>ADC-25</sub>, *bla*<sub>OXA-23</sub>, and *bla*<sub>TEM-1D</sub> in the *A. baumannii* AB329 genome. However, other beta-lactamase genes that were previously reported, such as *bla*<sub>PER-1</sub>, *bla*<sub>NDM-1</sub>, *bla*<sub>SPM</sub>, *bla*<sub>SIM</sub>, *bla*<sub>VIM</sub>, *bla*<sub>GIM</sub>, and *bla*<sub>IMP</sub>, were not detected in *A. baumannii* AB329 (Leungtongkam et al., 2018a; Hassan et al., 2021; Kongthai et al., 2021). In addition, four classes of efflux pumps, including the MFS, RND family, SMR family, and MATE family, are associated with the antimicrobial resistance of *A. baumannii* (Abdi et al., 2020). Consistent with a previous report, numerous virulence factors were detected in *A. baumannii* AB329 (Leal et al., 2020). Most of the virulence genes were detected in the other 292 *A. baumannii* strains isolated worldwide, and compared to the ARG patterns, the virulence gene patterns of XDRAB are not considerably different among the 292 *A. baumannii* strains (Figures 2A and 2B). These findings indicated that all *A. baumannii* strains were derived from the same ancestor

and employ the same pathogenic mechanisms for causing the disease. In contrast, horizontal gene transfer of ARGs is important for the difference in the ARG patterns, which leads to a critical problem in the treatment of *A. baumannii* infection.

Many of the virulence genes and ARGs are located in MGEs such as plasmids, GlS, transposons (Tn), and prophages. These elements can move between genomes through bacterial horizontal gene transfer (HGT). In this study, we detected pAB329b, a novel, non-characterized, 87 Kb plasmid. The genome structure of pAB329b is a conjugative plasmid and belongs to LN\_1 (*Salgado-Camargo et al., 2020*) classified in GR6 plasmid (*Bertini et al., 2010*). Some plasmids from this group contain ARGs such as *bla*<sub>oxa-23</sub> and are widespread, mainly in *A. baumannii* strains (*Bertini et al., 2010; Nigro & Hall, 2015*). Conjugation experiments demonstrated that amikacin resistance could be transferred from *A. baumannii* AB329 donors to sodium azide-resistant *A. baumannii* isolates, and *aph*(3')-VIa can be detected in the recipient. A previous study reported that the *bla*<sub>OXA-23</sub>, *bla*<sub>PER-1</sub>, and *aphA6* genes could be transferred between *A. baumannii* via the plasmid group GR6 or class 1 integrons (*Int1*) (*Leungtongkam et al., 2018b*). We were unable to find *Int1* as well as other classes (*Int2* and *Int3*) in the genome of *A. baumannii* AB329 which was consistent with a different study (*Ploy et al., 2000*).

Prophages are important MGEs that encode toxins, enzymes, or drug resistance genes that allow their host to become more virulent and contribute to the evolution of pathogenic bacteria. **In silico** analysis by Loh et al., 2020 identified numerous ARGs encoded for a beta-lactamase enzyme, N-Acetyltransferases, aminoglycoside phosphotransferases, and a macrolide efflux pump in 177 prophages identified in *A.*

*baumannii* genomes. However, we detected only the gene encoded for the MFS transporter in the genome of *A. baumannii* AB329. The presence of the MFS transporter was reported in the prophage of *A. baumannii* NCIMB8209, which is involved in DNA transport and necessary for biofilm formation (Repizo et al., 2020).

Accessory genes derived from HGT are found in typical regions known as GIs. Previous studies identified 63 GI loci in *A. baumannii*, and genes located within G4aby, G4abn, and G5abn were found to correspond to the resistance regions previously described as AbaR1, AbaR3, and AbaR4 (Di Nocera et al., 2011). AbaR4 was found in the genome of *A. baumannii* AB329. The AbaR4-type resistance island was the predominant type revealed to be a clone prevalent in most Asian countries; however, diverse variants of ARGs located within the island were found (Kim et al., 2012; Kim et al., 2013). An IS is a short DNA sequence that plays an extensive role in bacterial adaptation to antibiotic selective pressures. The previous study on 976 *A. baumannii* genomes detected 29 IS elements (Wright et al., 2017). ISAba1 is widely distributed in *A. baumannii* and plays a major role in the transfer and expression of *bla*<sub>OXA-23</sub> and *bla*<sub>ADC</sub> (Turton et al., 2006; Mugnier, Poirel & Nordmann, 2009; Joshi et al., 2017). In this study, 17 ISAba1 was detected in *A. baumannii* AB329 and found upstream/downstream of *ampC* and *bla*<sub>OXA-133</sub>. A previous report stated that the *bla*<sub>NDM-1</sub> gene was located within transposon Tn125 and bracketed by two copies of ISAba125. In this study, the *bla*<sub>NDM-1</sub> gene was found to be absent in *A. baumannii* AB329; however, ISAba125 was observed to be located upstream and downstream of *aph(3')-Ia* in pAB329b instead.

## Conclusions

In this study, we presented a whole genome analysis of *A. baumannii* AB329, XDRAB strain isolated from Thailand. The *A. baumannii* AB329 genome contained MGEs such as two plasmids, one intact prophage, 34 IS elements, and 19 GIs. Most ARGs were located in MGEs, suggesting that these MGEs are major mechanisms for the dissemination of ARGs in *A. baumannii*.

# **Acknowledgements**

We are grateful to Assoc. Prof. Dr. Jason Sahl and Watchanan Chantapakul for LS-BSR installation.

# References

1. Makke, G., Bitar, I., Salloum, T., Panossian, B., Alousi, S., Arabaghian, H., ... & Tokajian, S. (2020). Whole-genome-sequence-based characterization of extensively drug-resistant *Acinetobacter baumannii* hospital outbreak. *Mosphere*, 5(1), e00934-19.
2. Martins-Sorenson, N., Snesrud, E., Xavier, D. E., Cacci, L. C., Iavarone, A. T., McGann, P., ... & Moreira, B. M. (2020). A novel plasmid-encoded mcr-4.3 gene in a colistin-resistant *Acinetobacter baumannii* clinical strain. *Journal of Antimicrobial Chemotherapy*, 75(1), 60-64.
3. Salgado-Camargo, A. D., Castro-Jaimes, S., Gutierrez-Rios, R. M., Lozano, L. F., Altamirano-Pacheco, L., Silva-Sanchez, J., ... & Cevallos, M. A. (2020). Structure and evolution of *Acinetobacter baumannii* plasmids. *Frontiers in Microbiology*, 11, 1283.
4. Kongthai, P., Thummeepak, R., Leungtonkam, U., Pooarlai, R., Kitti, T., Thanwisai, A., ... & Sitthisak, S. (2021). Insight into molecular epidemiology, antimicrobial resistance, and virulence genes of extensively drug-resistant *Acinetobacter baumannii* in Thailand. *Microbial Drug Resistance*, 27(3), 350-359.
5. Saranathan, R., Sudhakar, P., Karthika, R. U., Singh, S. K., Shashikala, P., Kanungo, R., & Prashanth, K. (2014). Multiple drug resistant carbapenemases producing *Acinetobacter baumannii* isolates harbours multiple R-plasmids. *The Indian Journal of Medical Research*, 140(2), 262.
6. Leungtonkam, U., Thummeepak, R., Wongprachan, S., Thongsuk, P., Kitti, T., Ketwong, K., ... & Sitthisak, S. (2018a). Dissemination of bla OXA-23, bla OXA-24, bla OXA-58, and bla NDM-1 Genes of *Acinetobacter baumannii* Isolates from Four Tertiary Hospitals in Thailand. *Microbial Drug Resistance*, 24(1), 55-62.
7. Casjens, S. (2003). Prophages and bacterial genomics: what have we learned so far?. *Molecular microbiology*, 49(2), 277-300.
8. Loh, B., Chen, J., Manohar, P., Yu, Y., Hua, X., & Leptihn, S. (2020). A biological inventory of prophages in *A. baumannii* genomes reveal distinct distributions in classes, length, and genomic positions. *Frontiers in Microbiology*, 11, 3055.
9. Kim, D. H., Park, Y. K., & Ko, K. S. (2012). Variations of AbaR4-type resistance islands in *Acinetobacter baumannii* isolates from South Korea. *Antimicrobial Agents and Chemotherapy*, 56(8), 4544-4547.
10. Pagano, M., Martins, A. F., & Barth, A. L. (2016). Mobile genetic elements related to carbapenem resistance in *Acinetobacter baumannii*. *Brazilian Journal of Microbiology*, 47, 785-792.
11. Turton, J. F., Ward, M. E., Woodford, N., Kaufmann, M. E., Pike, R., Livermore, D. M., & Pitt, T. L. (2006). The role of IS Aba1 in expression of OXA carbapenemase genes in *Acinetobacter baumannii*. *FEMS Microbiology Letters*, 258(1), 72-77.
12. Bahador, A., Raoofian, R., Pourakbari, B., Taheri, M., Hashemizadeh, Z., & Hashemi, F. B. (2015). Genotypic and antimicrobial susceptibility of carbapenem-resistant *Acinetobacter baumannii*: analysis of ISAbA elements and blaOXA-23-like genes including a new variant. *Frontiers in Microbiology*, 6, 1249.
13. Joshi, P. R., Acharya, M., Kakshapati, T., Leungtonkam, U., Thummeepak, R., & Sitthisak, S. (2017). Co-existence of bla<sub>OXA-23</sub> and bla<sub>NDM-1</sub> genes of *Acinetobacter baumannii* isolated from Nepal: antimicrobial resistance and clinical significance. *Antimicrobial Resistance and Infection Control*, 6, 21.

14. Kim, D. H., Choi, J. Y., Kim, H. W., Kim, S. H., Chung, D. R., Peck, K. R., ... & Ko, K. S. (2013). Spread of carbapenem-resistant *Acinetobacter baumannii* global clone 2 in Asia and AbaR-type resistance islands. *Antimicrobial Agents and Chemotherapy*, 57(11), 5239-5246.
15. Bertini, A., Poirel, L., Mugnier, P. D., Villa, L., Nordmann, P., & Carattoli, A. (2010). Characterization and PCR-based replicon typing of resistance plasmids in *Acinetobacter baumannii*. *Antimicrobial Agents and Chemotherapy*, 54(10), 4168-4177.
16. Joshi, N.A., and J.N. Fass, others. (2011). Sickie: A sliding-window, adaptive, quality-based trimming tool for FastQ files (Version 1.33) [Software] Available from: <https://github.com/najoshi/sickle>.
17. Wick, R. R., Judd, L. M., Gorrie, C. L., & Holt, K. E. (2017). Unicycler: resolving bacterial genome assemblies from short and long sequencing reads. *PLoS Computational Biology*, 13(6), e1005595.
18. Seemann, T. (2014). Prokka: rapid prokaryotic genome annotation. *Bioinformatics*, 30(14), 2068-2069.
19. Kaas, R. S., Leekitcharoenphon, P., Aarestrup, F. M., & Lund, O. (2014). Solving the problem of comparing whole bacterial genomes across different sequencing platforms. *PloS One*, 9(8), e104984.
20. Liu, B., Zheng, D., Jin, Q., Chen, L., & Yang, J. (2019). VFDB 2019: a comparative pathogenomic platform with an interactive web interface. *Nucleic Acids Research*, 47(D1), D687-D692.
21. Sahl, J. W., Caporaso, J. G., Rasko, D. A., & Keim, P. (2014). The large-scale blast score ratio (LS-BSR) pipeline: a method to rapidly compare genetic content between bacterial genomes. *PeerJ*, 2, e332.
22. Yakkala, H., Samantarai, D., Gribskov, M., & Siddavattam, D. (2019). Comparative genome analysis reveals niche-specific genome expansion in *Acinetobacter baumannii* strains. *PLoS One*, 14(6), e0218204.
23. Johansson, M. H., Bortolaia, V., Tansirichaiya, S., Aarestrup, F. M., Roberts, A. P., & Petersen, T. N. (2021). Detection of mobile genetic elements associated with antibiotic resistance in *Salmonella enterica* using a newly developed web tool: MobileElementFinder. *Journal of Antimicrobial Chemotherapy*, 76(1), 101-109.
24. Arndt, D., Grant, J. R., Marcu, A., Sajed, T., Pon, A., Liang, Y., & Wishart, D. S. (2016). PHASTER: a better, faster version of the PHAST phage search tool. *Nucleic acids research*, 44(W1), W16-W21.
25. Fu, T., Fan, X., Long, Q., Deng, W., Song, J., & Huang, E. (2017). Comparative analysis of prophages in *Streptococcus mutans* genomes. *PeerJ*, 5, e4057.
26. Thummeepak, R., Pooalai, R., Harrison, C., Gannon, L., Thanwisai, A., Chantratita, N., ... & Sitthisak, S. (2020). Essential gene clusters involved in copper tolerance identified in *Acinetobacter baumannii* clinical and environmental isolates. *Pathogens*, 9(1), 60.
27. Di Nocera, P. P., Rocco, F., Giannouli, M., Triassi, M., & Zarrilli, R. (2011). Genome organization of epidemic *Acinetobacter baumannii* strains. *BMC Microbiology*, 11(1), 1-17.
28. Sullivan, M. J., Petty, N. K., & Beatson, S. A. (2011). Easyfig: a genome comparison visualizer. *Bioinformatics*, 27(7), 1009-1010.

29. Leungtongkam, U., Thummeepak, R., Tasanapak, K., & Sitthisak, S. (2018b). Acquisition and transfer of antibiotic resistance genes in association with conjugative plasmid or class 1 integrons of *Acinetobacter baumannii*. *PLoS One*, 13(12), e0208468.
30. Chopjitt, P., Wongsurawat, T., Jenjaroenpun, P., Boueroy, P., Hatrongjit, R., & Kerdsin, A. (2020). Complete genome sequences of four extensively drug-resistant *Acinetobacter baumannii* isolates from Thailand. *Microbiology Resource Announcements*, 9(40), e00949-20.
31. Si-Tuan, N., Ngoc, H. M., Nguyen, C., Pham, H. Q., & Huong, N. T. (2020). Genomic features, whole-genome phylogenetic and comparative genomic analysis of extreme-drug-resistant ventilator-associated-pneumonia *Acinetobacter baumannii* strain in a Vietnam hospital. *Infection, Genetics and Evolution*, 80, 104178.
32. Khuntayaporn, P., Kanathum, P., Houngsaitong, J., Montakantikul, P., Thirapanmethee, K., & Chomnawang, M. T. (2021). Predominance of international clone 2 multidrug-resistant *Acinetobacter baumannii* clinical isolates in Thailand: a nationwide study. *Annals of Clinical Microbiology and Antimicrobials*, 20(1), 1-11.
33. Chukamnerd, A., Singkhamanan, K., Chongsuvivatwong, V., Palittapongarnpim, P., Doi, Y., Pomwised, R., ... & Surachat, K. (2022). Whole-genome analysis of carbapenem-resistant *Acinetobacter baumannii* from clinical isolates in Southern Thailand. *Computational and Structural Biotechnology Journal*.
34. Silva, L., Grosso, F., Rodrigues, C., Ksiezarek, M., Ramos, H., & Peixe, L. (2021). The success of particular *Acinetobacter baumannii* clones: accumulating resistance and virulence inside a sugary shield. *Journal of Antimicrobial Chemotherapy*, 76(2), 305-311.
35. Hassan, R. M., Salem, S. T., Hassan, S. I. M., Hegab, A. S., & Elkholy, Y. S. (2021). Molecular characterization of carbapenem-resistant *Acinetobacter baumannii* clinical isolates from Egyptian patients. *Plos One*, 16(6), e0251508.
36. Abdi, S. N., Ghotaslou, R., Ganbarov, K., Mobed, A., Tanomand, A., Yousefi, M., ... & Kafil, H. S. (2020). *Acinetobacter baumannii* efflux pumps and antibiotic resistance. *Infection and Drug Resistance*, 13, 423.
37. Leal, N. C., Campos, T. L., Rezende, A. M., Docena, C., Mendes-Marques, C. L., de Sá Cavalcanti, F. L., ... & de-Melo-Neto, O. P. (2020). Comparative genomics of *Acinetobacter baumannii* clinical strains from Brazil reveals polyclonal dissemination and selective exchange of mobile genetic elements associated with resistance genes. *Frontiers in Microbiology*, 1176.
38. Nigro, S., & Hall, R. M. (2015). Distribution of the bla OXA-23-containing transposons Tn 2006 and Tn 2008 in Australian carbapenem-resistant *Acinetobacter baumannii* isolates. *Journal of Antimicrobial Chemotherapy*, 70(8), 2409-2411.
39. Ploy, M. C., Denis, F., Courvalin, P., & Lambert, T. (2000). Molecular characterization of integrons in *Acinetobacter baumannii*: description of a hybrid class 2 integron. *Antimicrobial Agents and Chemotherapy*, 44(10), 2684-2688.
40. Repizo, G. D., Espariz, M., Seravalle, J. L., Díaz Miloslavich, J. I., Steimbrüch, B. A., Shuman, H. A., & Viale, A. M. (2020). *Acinetobacter baumannii* NCIMB8209: a rare environmental strain displaying extensive insertion sequence-mediated genome remodeling resulting in the loss of exposed cell structures and defensive mechanisms. *Mosphere*, 5(4), e00404-20.
41. Wright, M. S., Mountain, S., Beerli, K., & Adams, M. D. (2017). Assessment of insertion sequence mobilization as an adaptive response to oxidative stress in *Acinetobacter baumannii* using IS-seq. *Journal of Bacteriology*, 199(9), e00833-16.

42. Mugnier, P. D., Poirel, L., & Nordmann, P. (2009). Functional analysis of insertion sequence IS Aba1, responsible for genomic plasticity of *Acinetobacter baumannii*. *Journal of Bacteriology*, 191(7), 2414-2418.

**Table 1. Genome features of the extensively drug-resistant *Acinetobacter baumannii* AB329**

Genome characteristics	AB329 (chromosome)	pAB329a (plasmid1)	pAB329b (plasmid2)
<b>General features</b>			
Genome size (bp)	3,948,038	8,731	82,120
Topology	circular	circular	circular
GC content (%)	39.0	34.4	33.7
Number of ORFs	3837	12	113
Number of CDSs	3747	12	113
Number of tRNAs	72	nd	nd
Number of rRNAs	18	nd	nd
In silico MLST (pasteur/oxford)	98/1166	nd	nd
<b>Insertion Sequences (ISs)</b>			
Number of total ISs	34	nd	3
Number of ISAba1	17	nd	1
Number of ISAba13	1	nd	nd
Number of ISAba24 (IS66)	1	nd	nd
Number of ISAba26	5	nd	nd
Number of ISAba33	9	nd	nd
Number of IS26(IS6)	1	nd	nd
Number of ISAba125	nd	nd	2
<b>Number of total prophage regions</b>			
Intact prophage	1	nd	nd
Incomplete prophage	2	nd	nd
<b>Genomic islands</b>			
Number of total genomic islands	8	nd	nd

nd: not detect

476 **Table 2. Conjugal transfer of the plasmid pAB329b and its contribution to**  
 477 **antibiotic susceptibility**

Characteristics	AB329	NU13R	NU13R-pAB329b
Conjugation frequency (CF)	-	-	$1.2 \times 10^{-7}$
Antibiogram	AK, CTX, CAZ, CRO, FEP, CIP, CN, IPM, MEM, TMX/SXT, TE, TZP	No resistance	AK
PCR-based plasmid GR typing	GR2, GR6	-	GR6
Aminoglycoside resistance genes	<i>aph(3')-VIa</i>	-	<i>aph(3')-VIa</i>



# Figure 1

Phylogenomic tree based on core-genome SNPs of *A. baumannii*

Phylogenomic tree based on core-genome SNPs of *A. baumannii* AB329 and 293 *A.baumannii* genomes deposited in the NCBI database (A) and comparative genomic analysis of the pan-genome identified in AB329 and its closely related genomes (B)

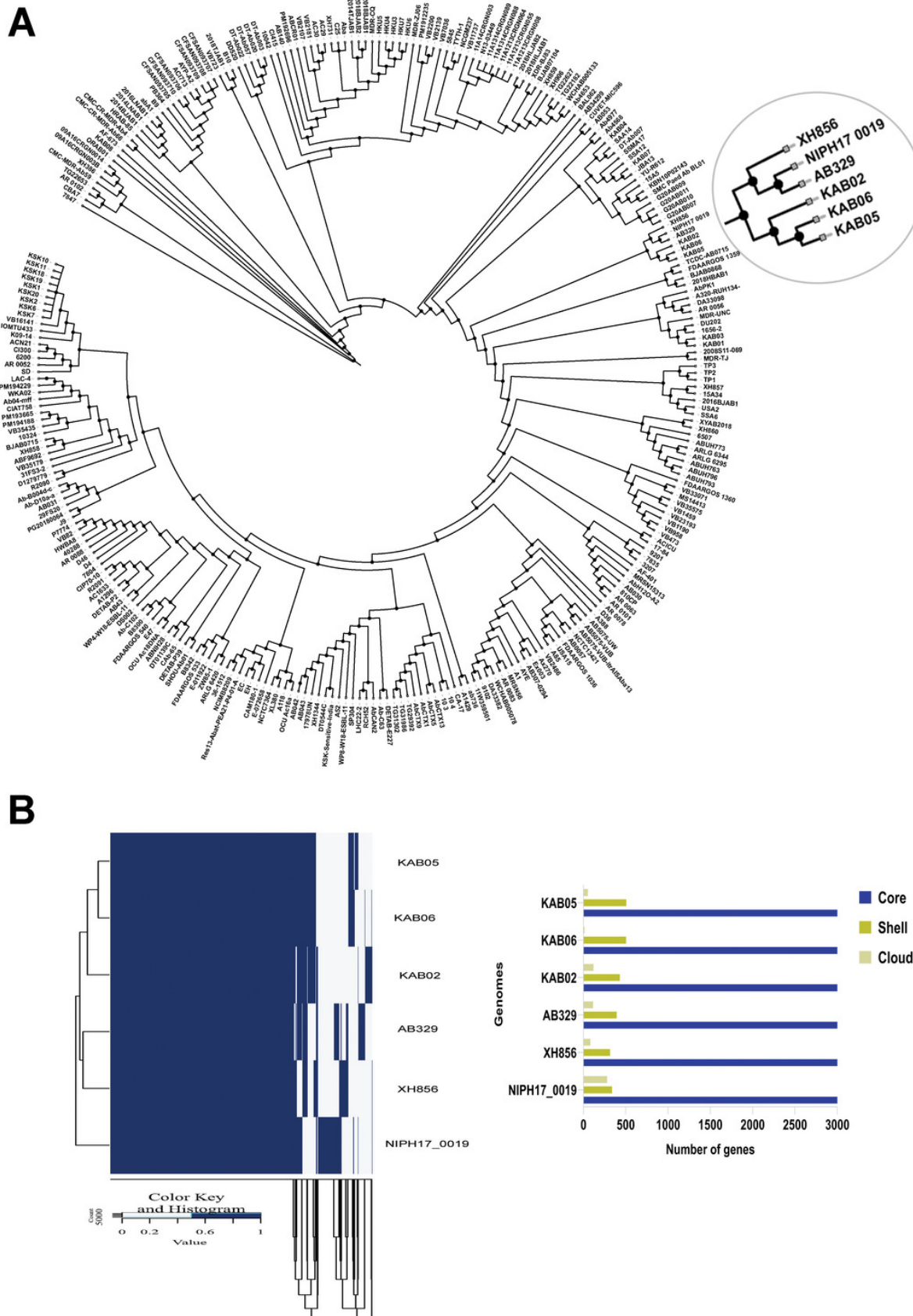


# Figure 2

Heatmap and antibiotic resistome of *A. baumannii* AB329

Heatmap showing LS-BSR analysis of virulome (A) and antibiotic resistome (B). *A. baumannii* AB329 was marked with a black triangle for virulome analysis while showing antibiotic resistome analysis in cluster C.

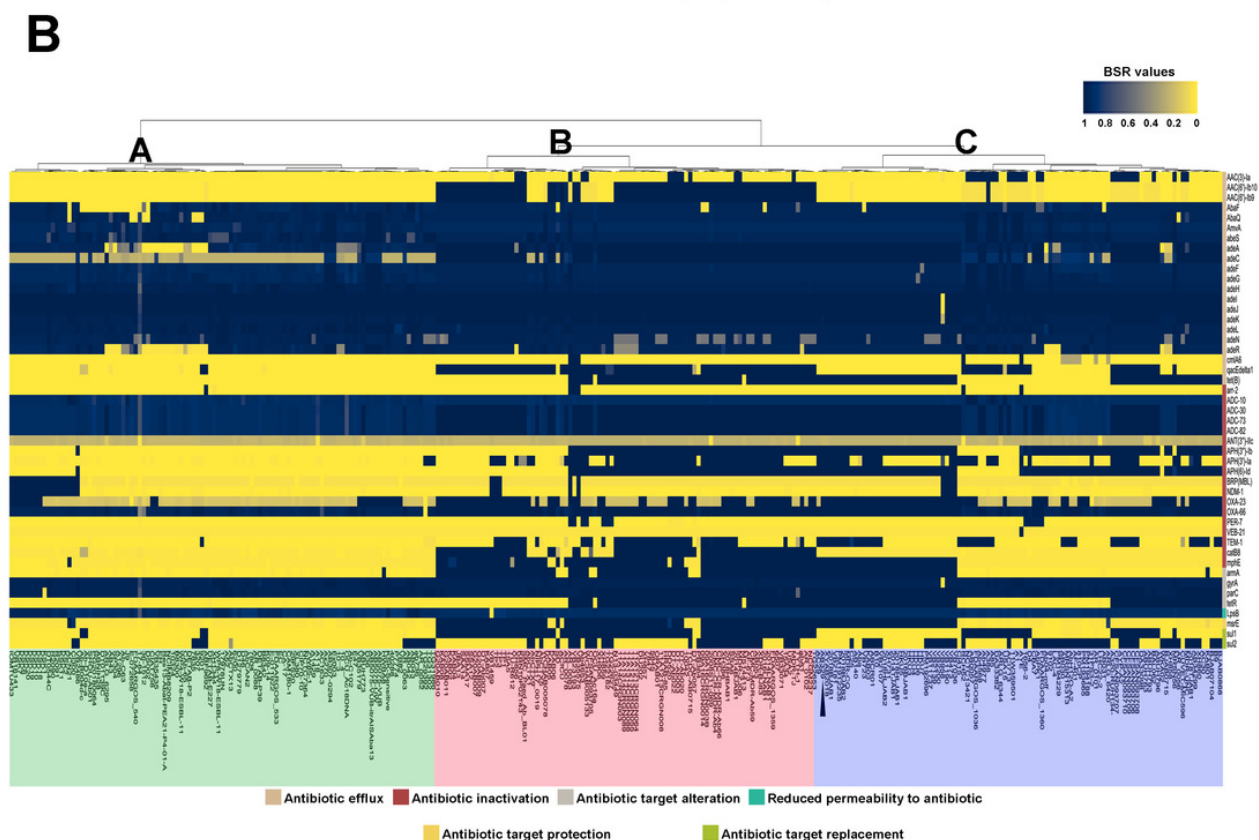
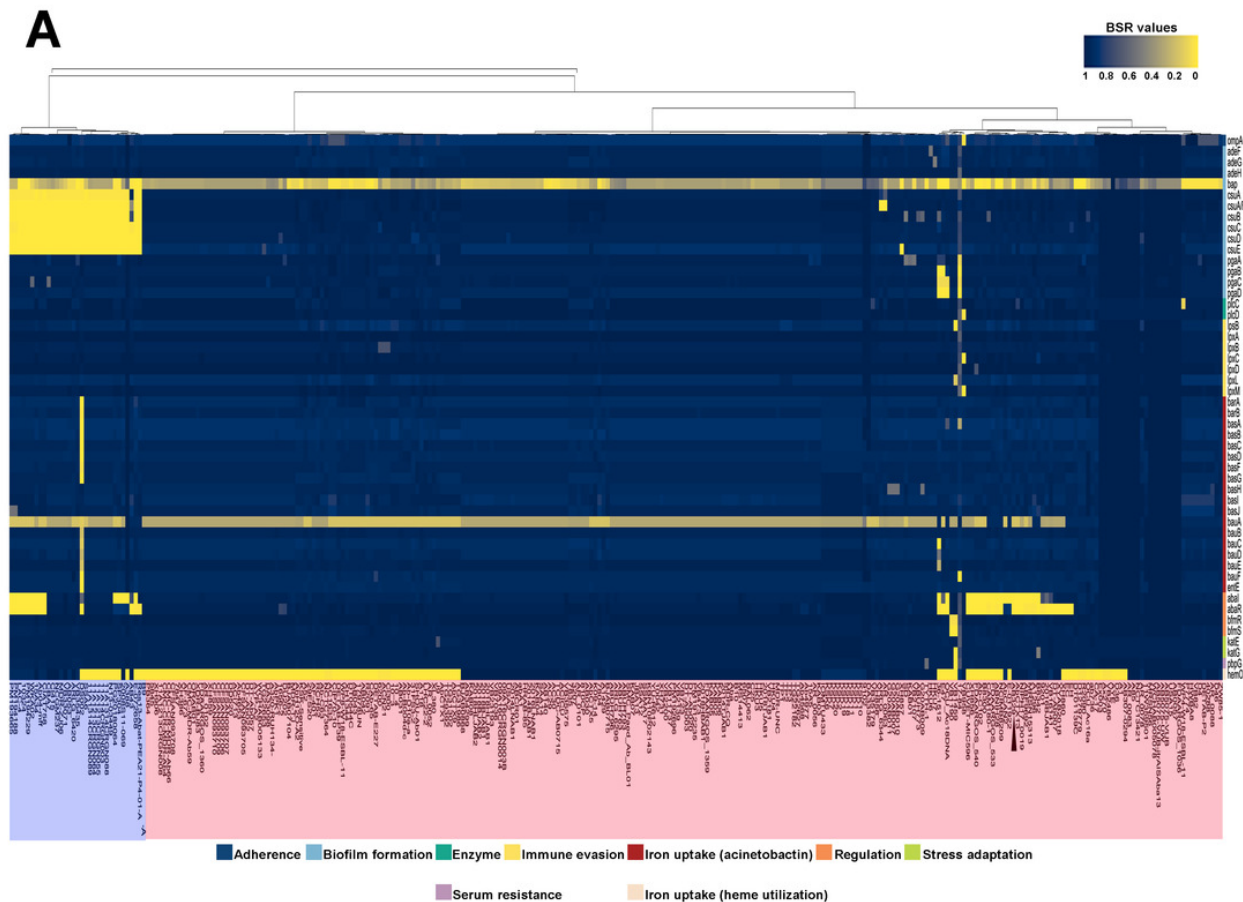
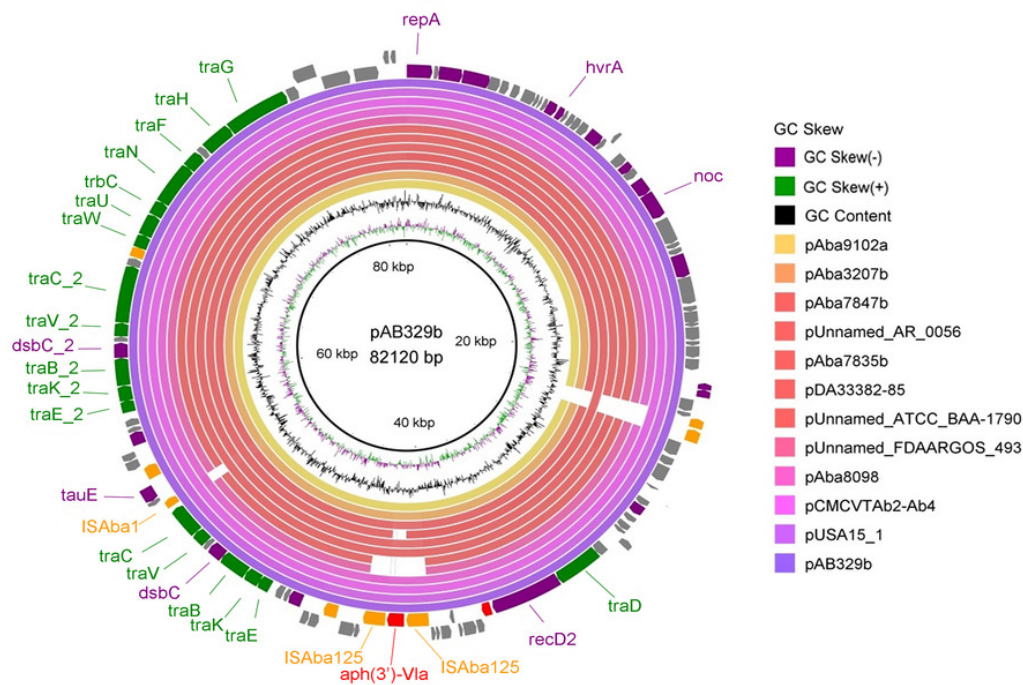


# Figure 3

Map of the conjugative plasmid pAB329b and backbone comparison between all regions of the plasmids pAB329b and pACICU2.

Circular map of the GR6 conjugative plasmid pAB329b and multiple plasmid comparisons with its 11 closely relative deposited in the GenBank database (A). The outer circle, ORFs, and their orientations are color-coded by functional category: navy: conserved hypothetical, green: Type IV secretion system (conjugation), red: drug- or putative virulence-associated proteins, orange: intact IS or transposase, and purple: plasmid replication, maintenance, or other functions. Backbone comparison between all regions of the plasmids pAB329b and pACICU2 (LN\_1) (B). Arrows represent the identified ORFs and are oriented in accordance with their direction. Homologous regions are highlighted in dark gray color, while the backbone regions are shown using yellow arrows.

A



B

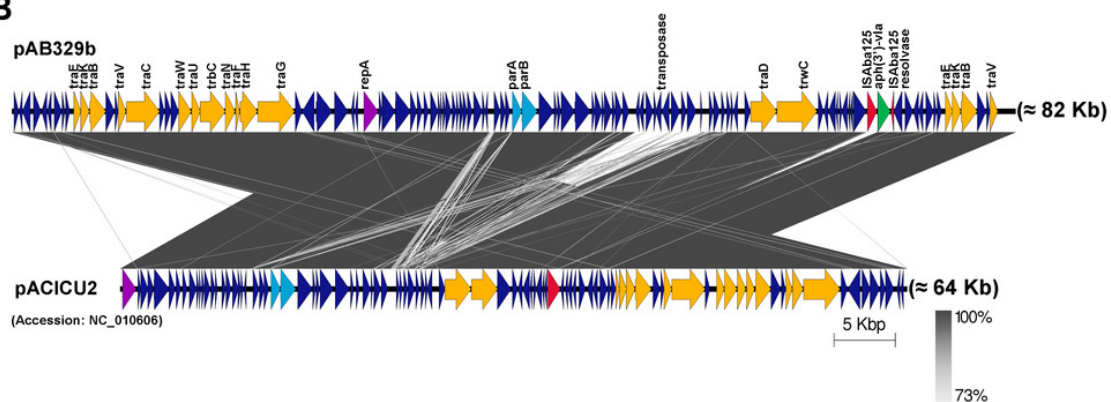
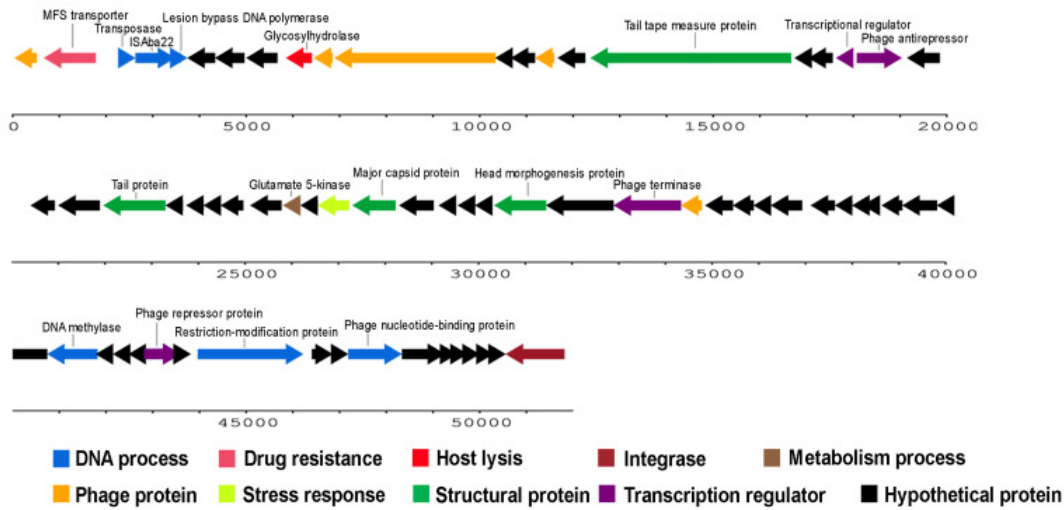


# Figure 4

Structure of intact prophage and AbaR4a identified in the *A. baumannii* strain AB329.

Genome organization of prophage within the AB329 (A) and comparison of genetic arrangement within AB329 with AbaR4a (LT-3) (GenBank: JN129845.1) derived from *A. baumannii* LT-3 (B).

A



B

